



ACADÉMIE
DES SCIENCES
INSTITUT DE FRANCE

Comptes Rendus

Chimie

Laurent Micouin and Erica Benedetti

Shaping the 3D architecture of [2.2]paracyclophanes: from selective functionalization to functional luminophores

Volume 28 (2025), p. 849-871

Online since: 24 November 2025

<https://doi.org/10.5802/crchim.423>



This article is licensed under the
CREATIVE COMMONS ATTRIBUTION 4.0 INTERNATIONAL LICENSE.
<http://creativecommons.org/licenses/by/4.0/>



*The Comptes Rendus. Chimie are a member of the
Mersenne Center for open scientific publishing*
www.centre-mersenne.org — e-ISSN : 1878-1543

Account

Shaping the 3D architecture of [2.2]paracyclophanes: from selective functionalization to functional luminophores

Laurent Micouin^{®,*} and Erica Benedetti^{®,*,a}^a Université Paris Cité, CNRS, Laboratoire de Chimie et de Biochimie
Pharmacologiques et Toxicologiques, F-75006 Paris, FranceE-mails: laurent.micouin@u-paris.fr (L. Micouin), erica.benedetti@u-paris.fr
(E. Benedetti)

Abstract. Over the past few years, [2.2]paracyclophanes (pCps) have attracted considerable attention due to their unique three-dimensional structure and distinctive electronic properties. In this account, we explore various strategies for selective modification of these molecules, with a particular focus on controlling their planar chirality and tuning their photophysical behavior. The versatility of pCps is further illustrated through their broad scope of applications, spanning the development of organic and organometallic luminophores, advances in photocatalysis, and contributions to biochemical research. These diverse applications underscore the strong potential of pCps as key platforms for the design of innovative molecular systems.

Keywords. [2.2]Paracyclophanes, Planar chirality, 3D luminophores, Organic photocatalysts, RNA ligands.

Funding. CNRS, Paris Cité University (IdEx Dynamique Recherche pCp-Photocat - ANR-18-IDEX-0001), Agence Nationale de la Recherche (ANR JCJC PhotoChiraPhane - ANR-19-CE07-0001-01).

Note. Article submitted by invitation.

Manuscript received 11 July 2025, revised 16 July 2025, accepted 12 September 2025.

1. Introduction

[2.2]Paracyclophane (pCp) is the smallest known member of the [n.n]cyclophane family. This molecule was serendipitously discovered and first isolated in 1949 by Brown and Farthing as an unexpected byproduct of the gas-phase pyrolysis of *para*-xylene [1]. X-ray diffraction analysis revealed that pCp consists of two benzene rings, commonly referred to as decks, arranged in a cofacial orientation and connected at the *para* positions by two ethylene bridges [2]. This molecular architecture forces the decks into an unusual boat-like conformation

(Figure 1), in which the bridgehead carbon atoms are displaced out of the plane defined by the remaining trigonal carbon atoms. Consequently, the distance between the carbon atoms bearing the ethylene bridges is shorter than the overall inter-ring separation (2.78 Å versus 3.09 Å, respectively, Figure 1).

These structural characteristics have a significant impact on the electronic distribution and chemical reactivity of the molecule, positioning pCp as a valuable scaffold for the design of novel aromatic compounds with a distinctive three-dimensional framework. Accordingly, significant research efforts have been dedicated to the synthesis and functionalization of pCp, as well as the modulation of its physicochemical properties and the exploration of its potential across various scientific domains [3].

*Corresponding author

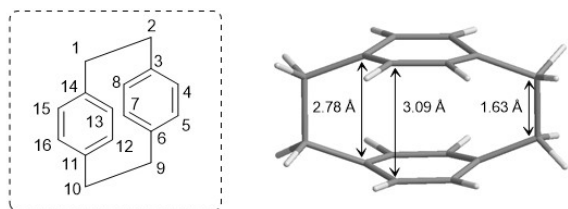


Figure 1. Structure of [2.2]paracyclophane (pCp).

In this account, we report our contributions to the chemistry of pCps, at first by placing our research in its broader context and outlining the strategies that we have developed to selectively functionalize the aromatic rings of commercially available pCp. Our methods for controlling the planar chirality inherent to these unique systems are then discussed. Finally, the synthesis of novel families of three-dimensional luminophores derived from pCp is described, and their applications across different research areas are discussed, including photocatalysis, coordination chemistry, and chemical biology.

2. Tailoring the aromatic decks of [2.2]paracyclophane

Since its discovery, numerous synthetic strategies have been developed to try and access pCp in an efficient manner. In addition to the industrial synthesis, which relies on the Hofmann elimination of *p*-methylbenzyl trimethylammonium hydroxide [4], the method reported by Brink in 1975 remains the most widely adopted and highest-yielding approach at the laboratory scale [5]. This approach involves the coupling of 1,4-bis(bromomethyl)benzene **1** with 1,4-bis(mercaptomethyl)-benzene **2** to produce dithia[3.3]paracyclophane **3**, followed by photochemical desulfurization to yield pCp in 51% overall yield (Scheme 1). This robust and reliable method has since enabled the synthesis of a broad range of pCp derivatives [6–8].

[2.2]Paracyclophanes are remarkably stable toward acids, bases, oxidants, or light, and retain their structural integrity up to 200 °C. Above this temperature, homolytic cleavage of the ethylene bridges occurs, leading to ring opening of the pCp core. This thermal behavior has been widely exploited in materials science, particularly for polymer production via chemical vapor deposition (CVD) processes [9–12].

For example, unsubstituted pCp is a key precursor in the synthesis of parylene (Scheme 1) [13], an aromatic polymer extensively used as a protective coating in electronics, optics, and biomedical devices.

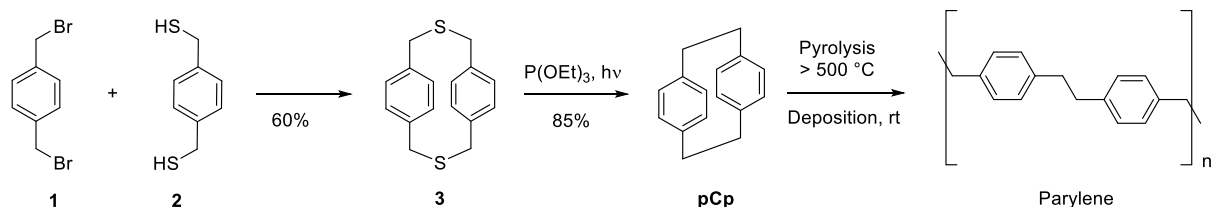
Owing to its widespread industrial applications, pCp is now commercially available at low cost. As a result, functionalized pCp derivatives are nowadays most easily prepared via direct functionalization of the parent compound, rather than through *de novo* synthesis of substituted analogues.

Each aromatic ring of the pCp scaffold offers four accessible positions, allowing up to eight possible sites for derivatization. Monofunctionalization is typically achieved through electrophilic aromatic substitution, enabling the introduction of diverse functions such as bromine atoms, formyl, nitro, or ester motifs. Alternatively, halogen–lithium exchange from brominated precursors followed by trapping with suitable electrophiles allows the incorporation of a broader array of functional groups, including amines, hydroxyls, azides, thiols, carboxylic acids, and phosphines [14]. More recently, direct C–H activation strategies have also emerged as effective tools for regioselective modification of the pCp core [15].

From monosubstituted intermediates, various disubstituted pCps can be easily prepared (Figure 2). These are typically classified according to their substitution pattern: *ortho*, *meta*, or *para* when both substituents are on the same aromatic ring; and *pseudo-gem*, *pseudo-ortho*, *pseudo-meta*, or *pseudo-para* when the substituents are located on both decks.

Higher substituted derivatives (tri- and tetrafunctionalized pCps) are generally synthesized via sequential electrophilic substitutions on di-substituted precursors [16]. However, systems bearing more than four substituents are highly strained and remain uncommon in the literature [17].

In certain cases, the reactivity of the aromatic units in pCps can pose notable synthetic challenges due to through-space electronic delocalization between the closely positioned π systems. Interestingly, reactivity patterns resembling those of isolated double bonds have been observed in some cases [18,19]. Moreover, the introduction of substituents on one deck can significantly influence the electronic distribution across the molecule, thereby activating or deactivating specific positions on the



Scheme 1. Synthesis and polymerization of [2.2]paracyclophane.

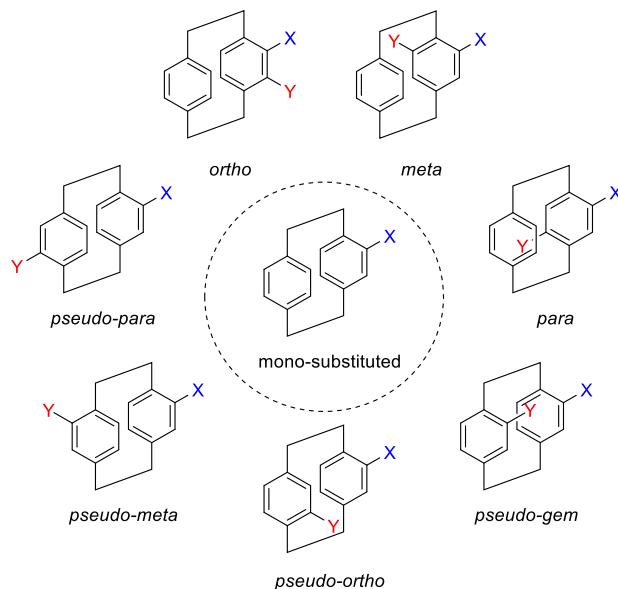


Figure 2. Substitution patterns and nomenclature of pCps.

opposite ring. For example, the introduction of electron-withdrawing groups can direct selective functionalization to the *pseudo-geminal* position, an effect well known and extensively exploited in [2.2]paracyclophane chemistry [20,21].

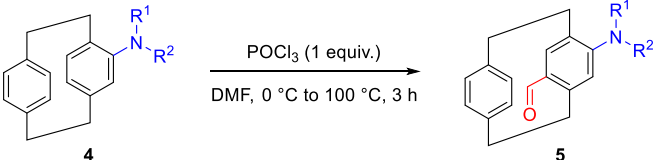
Despite significant progress, the selective introduction of multiple substituents onto a single aromatic ring of pCp remains a synthetic challenge. In our studies, we have developed an efficient and regioselective approach for synthesizing *para*-disubstituted pCps in a limited number of steps and with good overall yields. This strategy relies on a Vilsmeier–Haack formylation of various 4-amino[2.2]paracyclophane derivatives (**4**, Table 1), enabling the installation of a formyl group opposite to the existing electron-donating substituent.

The transformation is performed using POCl_3 (1 equiv.) in the presence of DMF, with the reaction mixture gradually heated from 0 to 100 °C over 3 h.

These conditions exhibit broad substrate tolerance, accommodating tertiary and secondary amines bearing alkyl, allyl, or benzyl substituents on the nitrogen atom, as well as derivatives featuring mildly electron-withdrawing groups, such as a 9-fluorenylmethyloxycarbonyl (Fmoc) motif (Table 1). This method provides access to a range of functionalized aldehydes in a practical and scalable manner, generating versatile intermediates for the construction of more elaborate molecular architectures based on the pCp core [22], as detailed in the following sections of this account.

3. Controlling planar chirality in [2.2]paracyclophanes

Extensive efforts have been devoted to the investigation and rationalization of the geometry of pCps.

Table 1. Para-formylation of 4-amino[2.2]paracyclophanes


Entry	Product	R ¹	R ²	Yield (%)
1	5a	Me	Me	90
2	5b	Bn	Bn	77
3	5c	H	Bn	72
4	5d	Allyl	Allyl	50
5	5e	H	Fmoc	42

For many years, it was believed that the unsubstituted pCp adopted a fully eclipsed conformation with D_{2h} symmetry. However, subsequent experimental and theoretical studies have shown that, at very low temperatures, the molecule favors a staggered conformation with D_2 symmetry, characterized by a torsional angle between 6 and 9°. As a result, the D_{2h} structure is now considered as a transition state between two enantiomeric D_2 conformers (Figure 3). Despite this, the unsubstituted pCp remains achiral at room temperature due to the rapid interconversion between its enantiomeric conformations [23–25].

Substituted pCps can exhibit planar chirality due to their rigid, strained structure, which prevents rotation of the aryl groups around their axes. Mono-substituted pCps are inherently nonsymmetrical, but disubstituted derivatives may or may not be chiral, depending on the nature and position of their substituents (Figure 3). Indeed, *ortho*, *meta*, *pseudo-gem*, and *pseudo-para* derivatives are achiral when both substituents are identical.

On the contrary, *para*, *pseudo-ortho*, and *pseudo-meta* pCps display planar chirality even when bearing the same substituents. A similar trend is observed for *tetra*-substituted derivatives (Figure 3) [14].

To assign the absolute configuration of pCps, specific Cahn–Ingold–Prelog rules (CIP conventions) [26] must be followed. The less substituted aromatic ring of the pCp core is positioned toward the front of the molecule, and the priority atom is identified as the carbon of the ethylene bridge bonded to the aromatic ring at the position nearest the highest-priority substituent. The configuration is

assigned by numbering the ring carbons beginning at the priority atom, moving sequentially toward the highest priority substituent, and including the aromatic quaternary carbon attached to the ethylene bridge. The direction of numbering (clockwise or counterclockwise) determines the R_p or S_p configuration, respectively (Figure 3).

Planar chirality in pCps was first identified by Gram and Allinger in 1955 [27]. Early research in this domain focused on synthesizing monosubstituted pCps and determining their absolute configuration. Since the 1990s, chiral pCps have become valuable ligands in asymmetric catalysis [28] and, more recently, key components in the development of circularly polarized light-emitting materials [29,30]. However, large-scale synthesis of polysubstituted pCps with controlled chirality remains a significant challenge, which still considerably limits their broader applications.

The synthesis of structurally complex enantiopure pCps typically involves the functionalization of simpler optically active intermediates. Over the years, various strategies have been developed to obtain such compounds in an efficient manner. Techniques like high-performance liquid chromatography (HPLC) on chiral stationary phases are commonly used for enantiomer separation, although they require costly equipment and large volumes of solvents. Classical resolution methods, which rely on forming diastereoisomeric products using stoichiometric amounts of chiral resolving agents, are also frequently employed to generate enantioenriched pCps. However, these approaches often involve multi-step syntheses (i.e., formation of

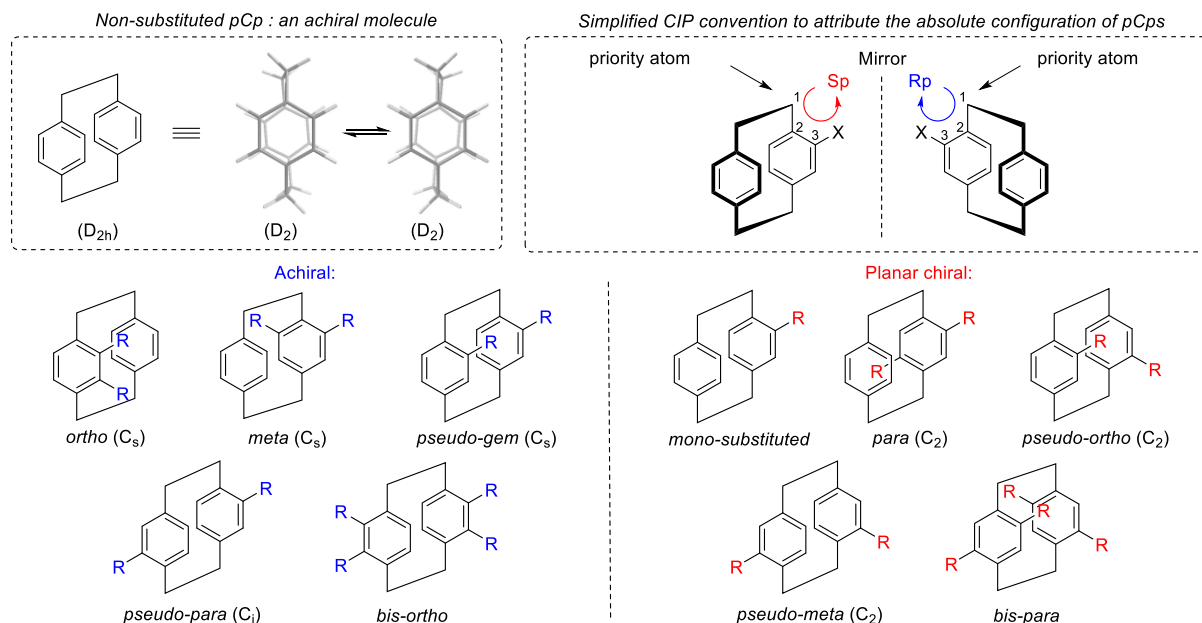


Figure 3. Achiral and planar chiral pCps.

the diastereomers, separation, and regeneration of the initial pCps), which are time-consuming [31].

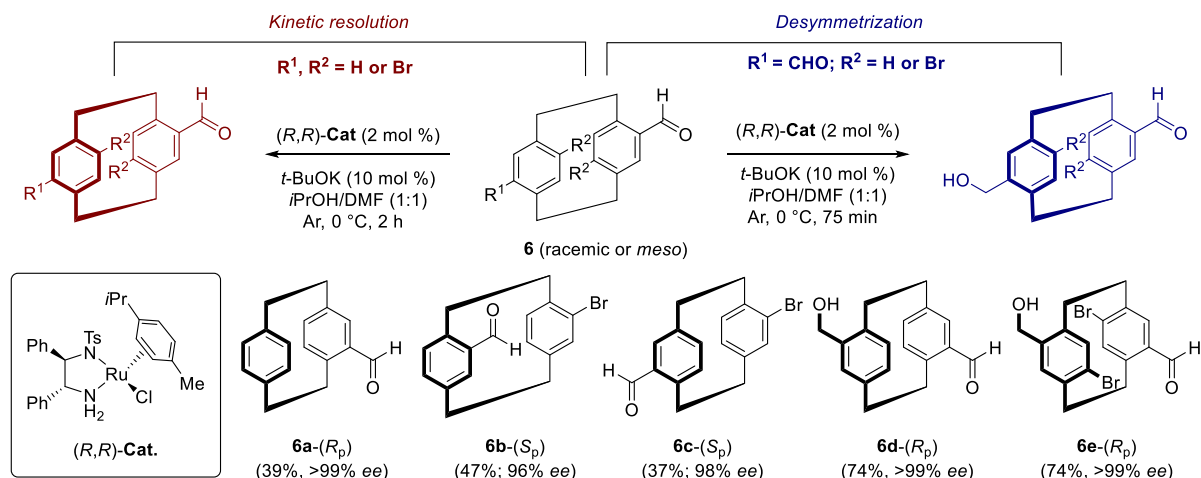
In our studies, we have investigated kinetic resolution and desymmetrization strategies as effective alternatives to traditional methods for accessing optically active pCps. Kinetic resolution (KR) constitutes a powerful approach wherein racemates undergo asymmetric transformations in the presence of a chiral catalyst, with the two enantiomers reacting at different rates. Ideally, at 50% conversion, one enantiomer is recovered as unreacted starting material, while the other one is obtained as the product. In contrast, desymmetrization of *meso* derivatives enables the generation of enantiopure compounds under similar catalytic conditions in yields up to 100%, by differentiating prochiral sites within an achiral molecule.

Starting from racemic aldehydes or centrosymmetric *meso* dialdehydes derived from pCp, we employed asymmetric transfer hydrogenations (ATH) as key transformations to control planar chirality [16,32,33]. After optimizing the reaction conditions, enantioselective reductions were successfully carried out using the commercially available Noyori's catalyst RuCl(*p*-cymene)[(R,R)-TsDPEN] ((R,R)-**Cat**,

1 mol%) in a 1:1 iPrOH/DMF mixture at 0 °C, with *t*-BuOK (5 mol%) as the base. These reactions, which are operationally simple and easy to implement, delivered a wide range of optically active products in short times (Scheme 2).

The resulting molecules possess diverse substituents, including carbonyl or hydroxyl groups, and halogen atoms, on each aromatic ring of the pCp core, thereby enabling further functionalization through a variety of orthogonal transformations such as condensations, nucleophilic substitutions, Grignard additions, transition-metal-catalyzed couplings, and olefination reactions. Enantiopure pCp-based aldehydes are thus now routinely prepared in our laboratory on multigram scales, serving as valuable key intermediates.

Notably, following our work, there has been a renewed interest in controlling the planar chirality of [2.2]paracyclophanes through catalytic chemical methods, resulting in a number of compelling contributions to the field [34–38]. Among the various strategies developed in this area, our approach has proven both viable and competitive, and it has been successfully employed by other research teams worldwide [39].



Scheme 2. Kinetic resolution and desymmetrization of aldehydes derived from [2.2]paracyclophanes.

4. Modulating the photophysical properties of [2.2]paracyclophanes

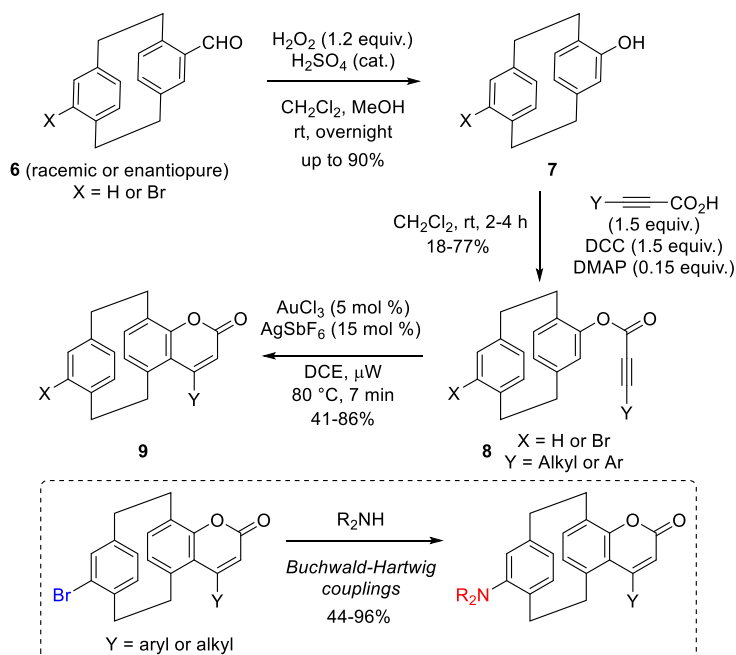
[2.2]Paracyclophanes are known to exhibit unique photophysical properties arising from electronic conjugation between their two aromatic rings, aided by both through-bond and through-space interactions. Indeed, unsubstituted pCp displays a distinctive UV–visible absorption spectrum, characterized by maxima at 225, 244, 286, and 302 nm [40,41]. The absorption band at the longest wavelength, commonly referred to as the cyclophane band, emerges in a spectral region that is atypical for standard benzene derivatives, such as xylenes. Furthermore, the molecule exhibits a broad fluorescence emission band centered around 356 nm. These characteristics have led to the widespread use of pCp as a core structure in the design of three-dimensional organic luminophores.

Pioneering studies have focused on the development of various systems that mimic excimers, transient dimers typically observed via fluorescence spectroscopy. In contrast to true excimers, which exist solely in the excited state, pCp-based analogues are stable in the ground state, making them particularly well-suited as model compounds for photophysical investigations. Notably, a variety of stilbene dimers incorporating the pCp scaffold have been isolated and thoroughly characterized [42–44]. Furthermore, di- and tetrasubstituted pCp derivatives bearing both electron-donating and electron-

withdrawing groups have been designed to probe through-space charge-transfer delocalization [45]. All these systems offer valuable insight into electronic communication between stacked aromatic units within the distinctive three-dimensional architecture of the pCp framework.

More recently, numerous studies have demonstrated that the synergistic interplay between planar chirality and the distinctive spectroscopic behavior of pCps can be effectively exploited for the development of advanced circularly polarized luminescence (CPL) emitters. Research on CPL active compounds has gained momentum, driven by their promising applications in advanced optoelectronic technologies, such as 3D displays, optical data storage, and bioimaging [46]. Nevertheless, the rational design of organic luminophores that combine high emission efficiency with strong chiroptical activity remains a major challenge, spurring ongoing innovation in molecular engineering.

In this context, helicene-like structures featuring a pCp core have been synthesized and extensively investigated for their CPL properties [47]. Additionally, a variety of second-order molecular architectures, such as V-, N-, M-, triangle-, propeller-, and X-shaped frameworks, have been constructed from pCp units [48–55]. These structurally complex compounds exhibit remarkable optical properties, including high molar extinction coefficients (ϵ), strong fluorescence with significant quantum yields (Φ), and impressive dissymmetry factors [56]



Scheme 3. Synthesis of pCp-based 3D coumarins.

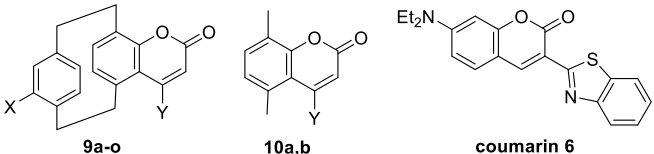
in both absorption (g_{abs}) and emission (g_{lum}). Such attributes render them promising candidates for the development of advanced functional materials in the field of chiral photonics.

As a complementary strategy to modulate the (chir)optical properties of pCps we explored the possibility of expanding the pCp aromatic framework to access functionalized polycyclic (hetero)aromatic derivatives—three-dimensional analogues of classical aromatic dyes such as naphthalenes, coumarins, and cyanines [57]. This approach has led to the development of chiral luminophores with more compact molecular structures and enhanced solubility, offering key advantages for solution-phase applications, including asymmetric catalysis, supramolecular recognition, and chiral sensing in complex environments.

All the new families of 3D luminescent compounds that we developed [57] were synthesized in just a few steps, starting from aldehyde intermediates, the chirality of which can be easily controlled using the methods described earlier in this article. For example, three-dimensional coumarin dyes were synthesized in three steps, beginning with Dakin oxidation, conducted using H_2O_2 and catalytic amount of H_2SO_4 in a $\text{CH}_2\text{Cl}_2/\text{MeOH}$ mixture, to

form 4-hydroxy[2.2]paracyclophanes **7** in up to 90% yield. These molecules were then esterified with various propiolic acid derivatives under classical conditions (DCC and DMAP cat. in CH_2Cl_2). The resulting esters **8** were subjected to cyclization promoted by gold- and silver-based catalysts in 1,2-dichloroethane under microwave irradiation at 80°C , yielding the desired coumarin core **9** (Scheme 3). In a final diversification step, starting from brominated compounds, Buchwald–Hartwig couplings were employed to introduce electron-donating amino groups on the pCp scaffold [58].

The impact of the pCp motif and its characteristic “phane” interactions on the spectroscopic properties of the synthesized coumarins was investigated using unpolarized UV–visible absorption and fluorescence spectroscopy. Overall, the three-dimensional dyes exhibited bathochromic shifts in both absorption and emission spectra compared to analogous planar structures (Table 2). Interestingly, the absorption maxima of the pCp-based coumarins remain hypsochromically shifted relative to those of planar commercial dyes such as **coumarin 6**, which possess a strong intramolecular charge-transfer character (Table 2). The luminescence properties of the 3D coumarins, which spanned the blue-to-green

Table 2. Spectroscopic properties of pCp-based coumarins and flat analogues


Entry	Compound	X, Y	$\lambda_{\max}^{\text{abs}}$ (nm)	$\lambda_{\max}^{\text{em}}$ (nm) ^d
1 ^a	9a	H, Ph	265, 300, 330	460
2 ^a	9b	H, Me	301, 319	435
3 ^a	9c	H, <i>i</i> Pr	300, 320	432
4 ^a	9d	H, H	304, 320	445
5 ^a	9e	Br, Ph	307, 325	450
6 ^a	9f	Br, Me	306, 320	425
7 ^a	9g	H, <i>p</i> -MePh	315	455
8 ^a	9h	H, <i>p</i> -OMePh	300, 330	455
9 ^a	9i	H, <i>p</i> -ClPh,	288, 310, 335	465
10 ^a	9j	H, <i>p</i> -OTfPh,	280, 330	470
11 ^a	9k	H, <i>p</i> -CF ₃ Ph	270, 335	475
12 ^a	9l	NHBoc, Ph	317	450
13 ^a	9m	NH ₂ , Ph	300, 330	560
14 ^a	9n	H, <i>p</i> -NHBocPh	317	450
15 ^a	9o	H, <i>p</i> -NH ₂ Ph	330	470
16 ^b	10a	-, Ph	294	418
17 ^b	10b	-, Me	286	413
18 ^c	Coumarin 6	-, -	455	498

^a10^{−4} M solution in 1,2-dichloroethane. ^b10^{−5} M solution in 1,2-dichloroethane.^c10^{−5} M solution in CH₂Cl₂. ^dNo significant effects were observed on the emission spectra while changing the excitation wavelength or the concentration of the samples.

region of the electromagnetic spectrum, were significantly influenced by the substitution pattern on the out-of-plane aromatic ring of the pCp core. In particular, the introduction of halogen atoms induced hypsochromic shifts in the emission profiles compared to their unsubstituted counterparts (Table 2, entries 5 and 6 versus entries 1 and 2). Conversely, amino-substituted derivatives bearing electron-donating groups exhibited pronounced bathochromic shifts in their emission maxima (Table 2, entry 13 versus entry 1), highlighting the effective modulation of luminescent properties through electronic effects. These findings clearly demonstrate that precise control over the photophysical behavior of these compounds can be achieved by

modulating both the nature and spatial arrangement of substituents around the three-dimensional pCp framework.

All pCp-based coumarins demonstrated notable photostability, along with exceptionally larger Stokes shifts (reaching up to 43 478 cm^{−1}) in comparison with their flat analogues. However, these dyes generally exhibited modest fluorescence quantum yields (0.1% < Φ < 5%).

In collaboration with Dr. J. Crassous's group, we carried out the chiroptical characterization of enantiopure planar chiral coumarins obtained from optically active aldehyde precursors [58]. As expected, electronic circular dichroism (ECD) spectra recorded in CH₂Cl₂ (10^{−5} M) displayed well-defined

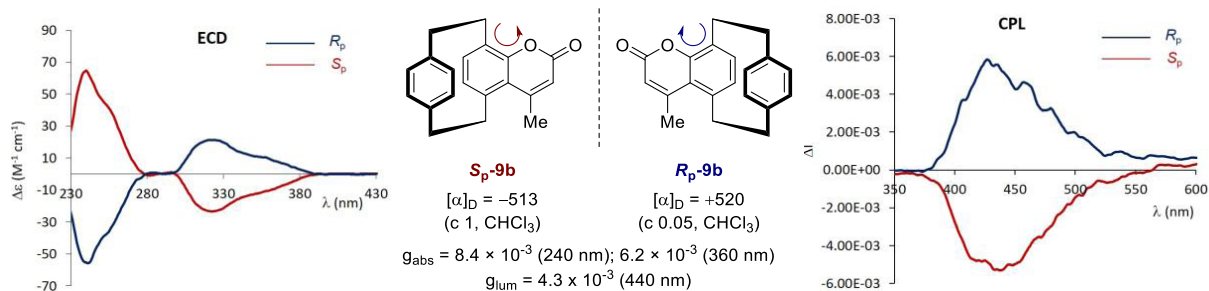


Figure 4. Chiroptical properties of pCp-based coumarins **Sp-9b** and **Rp-9b**. ECD and CPL spectra were recorded in CH_2Cl_2 (10^{-5} M, $\lambda_{\text{ex}} = 320$ nm).

mirror-image signatures for the two enantiomers of compound **9b** (Figure 4), with the **Sp** enantiomer exhibiting a strong positive Cotton effect at 240 nm ($\Delta\epsilon = +64 \text{ M}^{-1}\cdot\text{cm}^{-1}$) and a weaker negative one at 320 nm ($\Delta\epsilon = -23 \text{ M}^{-1}\cdot\text{cm}^{-1}$). Complementary CPL measurements under identical conditions ($\lambda_{\text{ex}} = 330$ nm) further revealed mirror-image emission profiles, consistent with their enantiomeric nature (Figure 4). Overall, the pCp-based coumarin derivatives showed promising chiroptical responses, with dissymmetry factors of $g_{\text{abs}} \approx 6.2 \times 10^{-3}$ at 360 nm and $g_{\text{lum}} \approx 4.0 \times 10^{-3}$ at 440 nm. These values are especially noteworthy given the compact and rigid nature of the molecular framework in contrast to the previously reported systems based on extended π -conjugation. Additionally, the $g_{\text{lum}}/g_{\text{abs}}$ ratio of ~ 0.7 suggests minimal structural reorganization upon excitation, an advantageous feature for preserving chiroptical integrity in emissive applications.

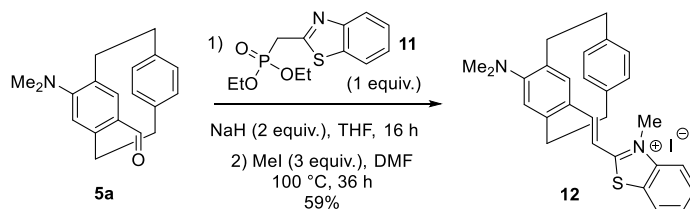
Three-dimensional cyanine-type dyes based on the pCp scaffold were also readily prepared from aldehyde intermediates, particularly those obtained via the regioselective formylation strategy outlined in Table 1. In this case, key aldehyde **5a**, bearing a dimethylamino group, underwent a Wittig-type reaction with compound **11**, followed by *N*-methylation of its benzothiazole moiety. This sequence efficiently led to the formation of novel luminescent compound **12**, which exhibited emission in the red region of the electromagnetic spectrum (Scheme 4). Once again, both racemic and enantiopure products could be synthesized using the strategies developed in our laboratory [59].

The photophysical properties of three-dimensional cyanine dye **12** were investigated in both

dichloromethane and an aqueous Tris-EDTA (TE) buffer, the latter containing 1% DMSO to ensure full solubilization of the organic compound. When comparing the two environments, a modest hypsochromic shift in both absorption and emission maxima was observed upon transitioning from the organic to the aqueous medium (Table 3). Additionally, both the molar extinction coefficient and fluorescence quantum yield were reduced in the TE buffer, indicating diminished brightness in the aqueous phase.

Compared to its flat analogue **13** [60], pCp-based cyanine **12** exhibited significantly red-shifted absorption and emission spectra in both organic and aqueous media (Table 3). This pronounced bathochromic shift aligns with observations made for other pCp-derived fluorophores, including the coumarin chromophores discussed earlier. This effect is attributed to the presence of the second aromatic ring in the pCp scaffold, which serves as a mild electron-donating group, thereby modulating the global electronic properties of the dyes.

Overall, these results underscore the remarkable versatility of pCp-based three-dimensional luminophores. By tailoring the functionalization of the pCp core, we can precisely tune absorption and emission profiles to cover the entire visible spectrum and develop differently colored CPL emitters from enantiopure molecules [57]. The diverse families of compounds we have isolated hold promise for a wide range of applications in different domains, including coordination chemistry, photocatalysis, and the chemistry–biology interface. Their potential in these areas will be explored in greater detail in the following sections.



Scheme 4. Synthesis of a pCp-based 3D cyanine.

Table 3. Spectroscopic properties of cyanine dyes in different media

Dye ^a	Solvent	$\lambda_{\text{abs}}^{\text{max}}$ (nm)	ϵ_{max} ($\text{M}^{-1} \cdot \text{cm}^{-1}$)	$\lambda_{\text{em}}^{\text{max}}$ (nm)	Φ_f (%) ^b
12	CH_2Cl_2	597	46×10^3	645	2.0
	TE^c	565	39×10^3	635	1.5
13	CH_2Cl_2	553	44×10^3	607	6.2
	TE^c	510	36×10^3	600	1.3

^a 10^{-5} M solution. ^bAbsolute quantum yields. ^c1% DMSO was added to fully solubilize the dyes.

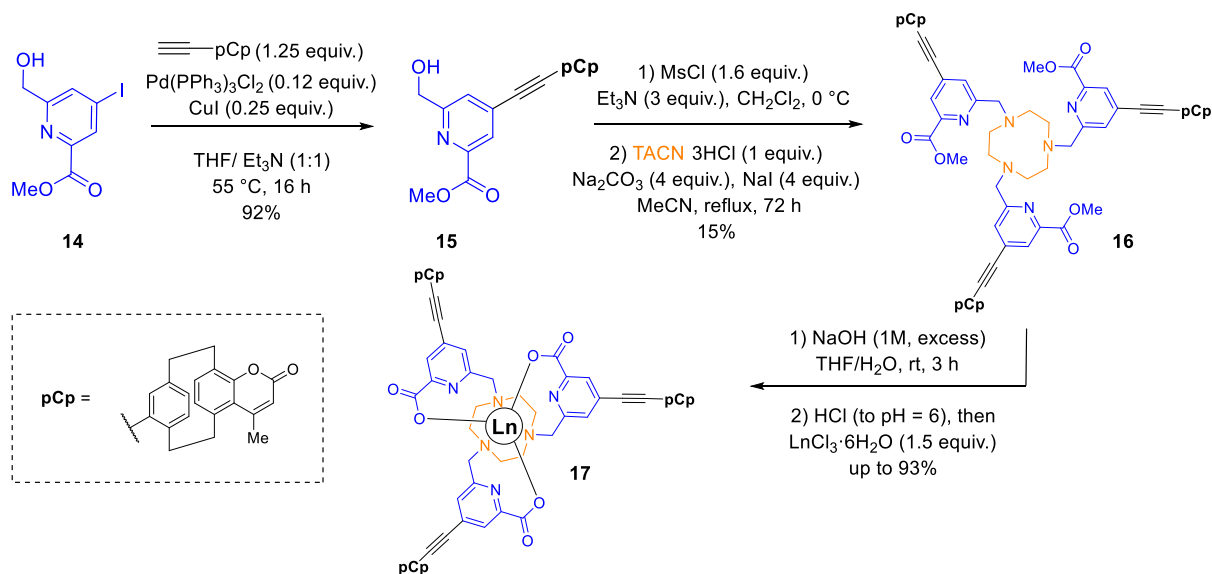
5. Lanthanide luminescence sensitization using [2.2]paracyclophanes

In recent decades, the distinctive photophysical characteristics of lanthanide ions (Ln) have garnered considerable interest, owing to their sharp emission bands and prolonged luminescence lifetimes [61], which make them particularly attractive for imaging and photonic applications [62–64]. In addition, lanthanide-based organometallic complexes exhibit exceptional photostability, effectively addressing a major limitation of conventional organic fluorophores, namely, photobleaching under prolonged or intense light exposure. A key limitation, however, arises from the intrinsically low molar absorption coefficients of lanthanide cations ($\epsilon < 1 \text{ M}^{-1} \cdot \text{cm}^{-1}$), which severely restricts their direct excitation. To circumvent this issue, the use of antenna ligands, chromophores capable of efficiently absorbing light and transferring the harvested energy to the lanthanide

center, has become a widely adopted strategy for efficiently sensitizing lanthanide emission [65,66].

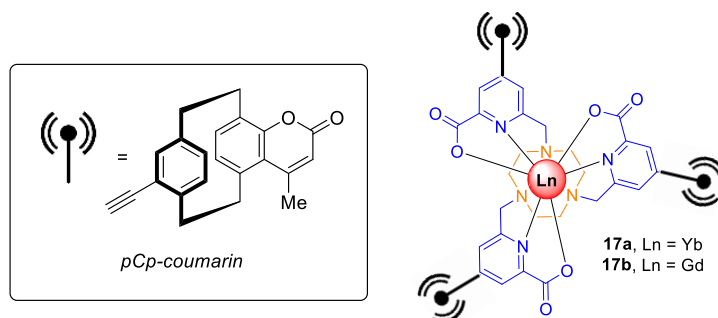
In this context, our group has investigated the potential of luminophores derived from pCp as antenna or ligands for lanthanide sensitization. While pCps have demonstrated significant utility in transition metal coordination chemistry [67], their application in lanthanide systems, either as antennas or as coordinating ligands, remains largely unexplored to date [68]. We thus identified a promising opportunity to expand the functional utility of pCp-based scaffolds by designing new Ln–pCp complexes with enhanced photophysical performance.

As part of this study, in collaboration with Dr. O. Maury's group (ENS Lyon), we successfully prepared a series of picolinate-based lanthanide complexes bearing pCp-derived coumarin antennas (Scheme 5) [69]. The synthesis of these molecular objects began with compound **15**, obtained from a 3D coumarin bearing a triple bond at its *pseudo-para*



Scheme 5. Synthesis of Ln complexes incorporating pCp-based coumarins as antennas.

Table 4. Photophysical properties of Ln complexes **17a** and **17b**



Ln	λ_{abs} (nm) ^a	ϵ (L·mol ⁻¹ ·cm ⁻¹)	λ_{em} (nm) ^a	τ_{obs} (μs) ^a	Φ^b	Φ_{Δ}^c
17a	332	48.5×10^3	980	9.48	<0.01	0.00
17b	332	61×10^3	422	-	<0.01	0.45

^aSolution in CH₂Cl₂ (10⁻⁵ M); ^bfluorescence quantum yield; ^cquantum yield for singlet oxygen generation.

position, via a Sonogashira cross-coupling with iodo-picolinic ester **14**. Following mesylation, the intermediate was coupled to 1,4,7-triazacyclononane (TACN), yielding target ligand **16** in 15% overall yield after purification by column chromatography. Complexation with lanthanide ions was then carried out via in-situ saponification, followed by the addition of the hydrated lanthanide chloride at pH 6 (Scheme 5).

Spectroscopic characterization revealed that the pCp-coumarin unit undergoes rapid intersystem crossing from the singlet to the triplet excited state [$E(T_1) = 19\,500\text{ cm}^{-1}$]. The triplet-state energy is well-matched for efficient energy transfer to Yb³⁺ and Gd³⁺ ions. This was confirmed by excitation of the antenna at 332 nm, which resulted in the characteristic near-infrared (NIR) luminescence of Yb³⁺ in complex **17a** ($\lambda_{\text{em}} = 980\text{ nm}$, Table 4, entry 1).

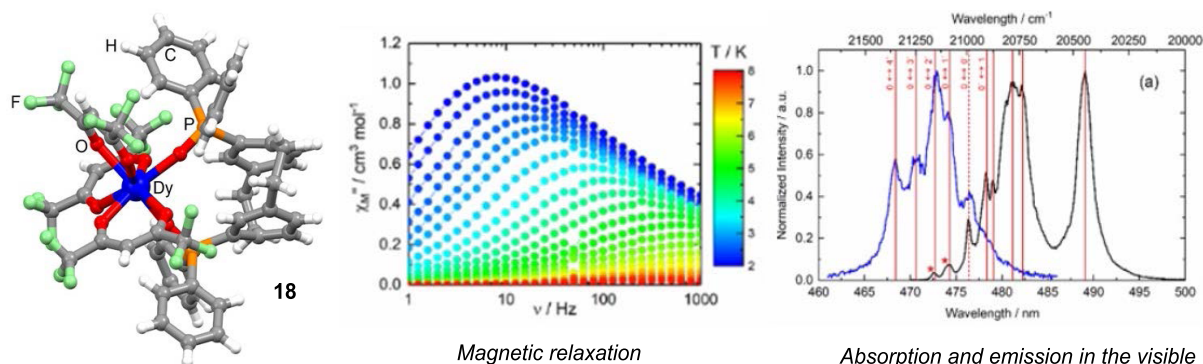


Figure 5. Luminescence and magnetic properties of a Dy(III) complex incorporating a pCp-based ligand.

Notably, under the same excitation conditions, Gd^{3+} -containing complex **17b** was found capable of generating a singlet oxygen, with a quantum yield of $\Phi_{\Delta} = 0.45$ (Table 4, entry 2) [69]. These findings highlight the potential of pCp-based architectures for the development of lanthanide complexes with tunable and multifunctional properties [70].

Lanthanide ions are currently the focus of extensive research in the field of molecular magnetism [71], as they are prime candidates for the design of single-molecule magnets (SMMs). Unlike traditional magnets, which consist of large assemblies of atoms, SMMs are composed of discrete mono-, di-, or polynuclear complexes capable of retaining magnetic information at low temperatures [72]. To fully harness the potential of SMMs for practical use, it is crucial to investigate their magnetic properties in relation to other physical characteristics, such as luminescence and chirality. This could pave the way for multifunctional materials in emerging technologies, such as: quantum computing, where the integration of stable magnetic states and optical properties could lead to more reliable qubits; molecular electronics, where combining magnetic and luminescent properties may improve device performance and enable further miniaturization; and high-density data storage, where the ability to manipulate and store information at the molecular level could transform data retention capabilities. In this context, luminescent SMMs based on lanthanide complexes, incorporating ligands with central, axial, or helical chirality, have been developed [73]. Embedding rare-earth ions within chiral organic frameworks facilitates chirality transfer

from the ligand to the metal center, generating circular anisotropies at the lanthanide ion level. This can give rise to phenomena such as CPL and magnetochiral dichroism (MChD) [74]. Surprisingly, planar chiral ligands have yet to be utilized to modulate these intriguing properties in lanthanide complexes.

Recently, in collaboration with Dr. O. Maury (ENS Lyon) and Dr. F. Pointillart (Univ. Rennes 1), we employed racemic pCp-derived phosphine oxides as ligands to finely tune the crystal field and electronic environment surrounding Yb^{3+} and Dy^{3+} ions, thereby enabling the manifestation of slow magnetic relaxation (Figure 5). The synthesized complexes also exhibited distinct luminescence in the visible or NIR regions of the electromagnetic spectrum. A magneto-structural correlation between the emission and magnetic properties was established for these new complexes, thereby contributing to a deeper understanding of the interplay between these phenomena [75].

Our laboratory is currently exploring the use of enantiopure pCps as antennas or ligands for lanthanide ions, with the objective of developing novel multifunctional molecular systems that integrate luminescence, magnetism, and planar chirality.

6. [2.2] Paracyclophanes as building blocks for the design of organic photocatalysts

At the beginning of the last century, Ciamician recognized that visible light could serve as a renewable and cost-effective energy source for driving chemical reactions under mild and environmentally friendly

conditions [76]. Since then, the fields of photochemistry and photocatalysis have unveiled numerous opportunities for reimagining established reactions and pioneering pathways to previously inaccessible products [77]. Over the years, a variety of highly performant photocatalytic systems have been developed, ranging from metal-based compounds such as ruthenium and iridium polypyridyl complexes to fully organic molecules like eosin Y or acridinium salts. Despite these inspiring advances, the quest continues for novel, more versatile molecules capable of promoting a broader range of catalytic photoreactions. Regardless of their intriguing photophysical properties and considerable potential, pCps had remained largely unexplored as catalysts in photochemical transformations until very recently [39].

As a proof of concept, and inspired by previous reports [78–80], our group demonstrated that pCp-based coumarins can serve as organic photocatalysts, effectively promoting desulfonylation reactions under light irradiation [81].

Starting from a readily accessible model substrate (**19a**, Table 5), prepared according to a reported procedure [78], coumarin derivative **9b** demonstrated effective photocatalytic activity for the reductive cleavage of the tosyl protecting group. Using a Hantzsch ester as the sacrificial electron donor, irradiation at 300 nm led to 65% conversion within 2 h (Table 5, entry 1). Prolonging the reaction time did not improve this outcome (Table 5, entry 2); however, catalyst loading could be reduced from 20 to 5 mol% without any loss in efficiency (Table 5, entries 3 and 4). A series of structurally related pCp-based coumarins was evaluated to probe structure–activity relationships. Interestingly, catalyst **9a** bearing aryl substituents proved significantly less effective (Table 5, entry 7), indicating that an alkyl group on the coumarin framework may be crucial for efficient photocatalysis in this case. Control experiments further confirmed the key roles of each component: no conversion was observed in the dark or in the absence of the Hantzsch ester (Table 5, entries 8 and 9), while reactions conducted without the pCp-coumarin—or with pCp-deprived analogue **10b**—resulted in only traces of conversion (Table 5, entries 10 and 11). These findings underscore the unique contribution of the pCp moiety to the activity of the photocatalyst. The presence of oxygen significantly suppressed the deprotection (Table 5,

entry 12), and no conversion was observed when TEMPO, a well-established radical scavenger, was added to the reaction mixture (Table 5, entry 13). Alternative reducing agents were evaluated as well but did not exhibit performances comparable to the Hantzsch ester (Table 5, entries 14–16).

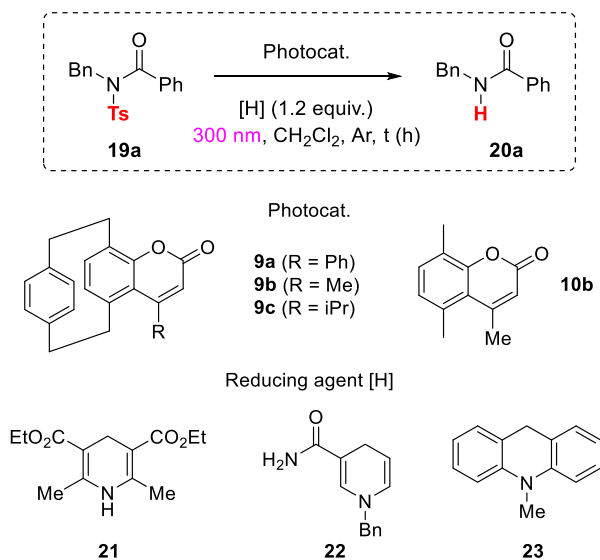
The scope of the reaction was subsequently examined using the conditions optimized on substrate **19a**, as illustrated in Scheme 6. The deprotection of a range of sulfonyl groups, including tosyl (Ts), phenylsulfonyl (SO₂Ph), and mesitylsulfonyl (SO₂Mes), was tested using 5 mol% of catalyst **9b**. In line with the reactivity observed for the Ts group, efficient removal of the phenylsulfonyl moiety afforded compound **20a**³ in 59% yield. Conversely, sulfonamides bearing mesityl or mesyl groups proved unreactive under identical conditions, yielding only trace amounts of the desired product.

Substrates containing tosyl groups with a variety of functional motifs, such as substituted (hetero)arenes, alkyl chains, and a Boc-protected amine, were well tolerated, affording the corresponding products in good yields. The method also extended to sulfonamides incorporating alternative aroyl groups, although substrates bearing electron-donating substituents showed reduced efficiency (Scheme 6).

Notably, the protocol was compatible with stereochemically sensitive compounds. When enantiomerically enriched substrates were subjected to the reaction conditions, the corresponding products were obtained with full retention of enantiopurity. This indicates that the transformation proceeds without racemization, even in the presence of base-sensitive stereogenic centers (Scheme 6).

It is worth highlighting that the presence of an aroyl group on the sulfonamide was critical for successful cleavage. Substrates featuring alternative groups such as acetyl, Boc, or methyl failed to undergo transformation under the optimized conditions (Scheme 6).

To gain deeper insight into the mechanism of the photodesulfonylation promoted by pCp-based coumarins, we conducted a series of mechanistic studies. Computational analysis realized in collaboration with A. Maruani (LCBPT UPCit ) revealed that energy transfer (EnT) from the excited state of catalyst **9b** to the lowest excited state of substrate **19a** is thermodynamically uphill ($\Delta G_{\text{EnT}} = +1.13$ eV), rendering this pathway unlikely. Based on prior studies

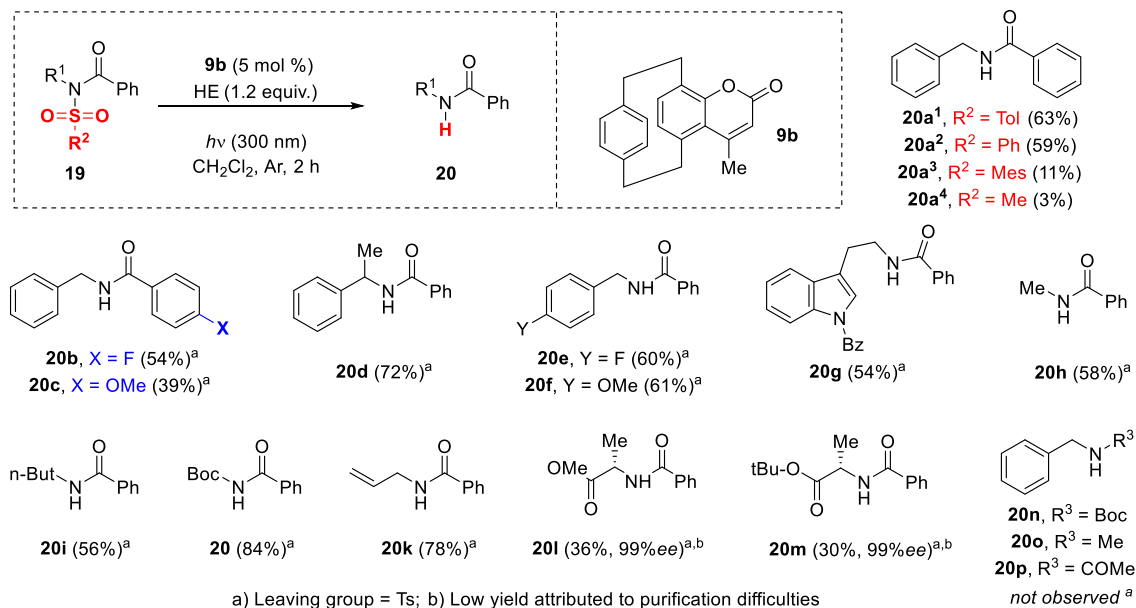
Table 5. Optimization of the photodeprotection reaction

Entry	Photocat. (mol%)	[H]	<i>t</i> (h)	Conv. (%) ^e
1	9b (20)	21	2	66
2	9b (20)	21	16	71
3	9b (15)	21	2	63
4	9b (5)	21	2	65
5 ^a	9b (5)	21	2	64
6	9c (5)	21	2	56
7	9a (5)	21	2	26
8 ^b	9b (5)	21	2	-
9	9b (5)	-	2	-
10	-	21	2	9
11	10b (5)	21	2	14
12 ^c	9b (5)	21	2	19
13 ^d	9b (5)	21	2	-
14	9b (5)	22	2	-
15	9b (5)	23	2	-
16	9b (5)	<i>n</i> -Bu ₄ NBH ₄	2	-

Reactions were performed in a Rayonet photochemical reactor equipped with eight 300 nm lamps ($T = 29\text{ }^{\circ}\text{C}$, $c = 0.05\text{ M}$). ^aReaction performed under more diluted conditions ($c = 0.025\text{ M}$); ^breaction performed in dark ($T = 25\text{ }^{\circ}\text{C}$, $c = 0.05\text{ M}$); ^creaction performed under an oxygen atmosphere; ^dreaction performed in the presence of TEMPO (1 equiv.); ^edetermined by ¹H NMR analysis.

involving an iridium-based photocatalyst combined with a Hantzsch ester [78], we hypothesized that the sulfonamide cleavage could proceed via a photoinduced electron transfer (ET) mechanism.

Electrochemical measurements of the redox potentials of **9b**, **19a**, and **21**, combined with the determination of the excited-state energy (E^*) of **9b** via absorption and fluorescence spectroscopy, enabled



Scheme 6. Scope of the photodesulfonylation reaction.

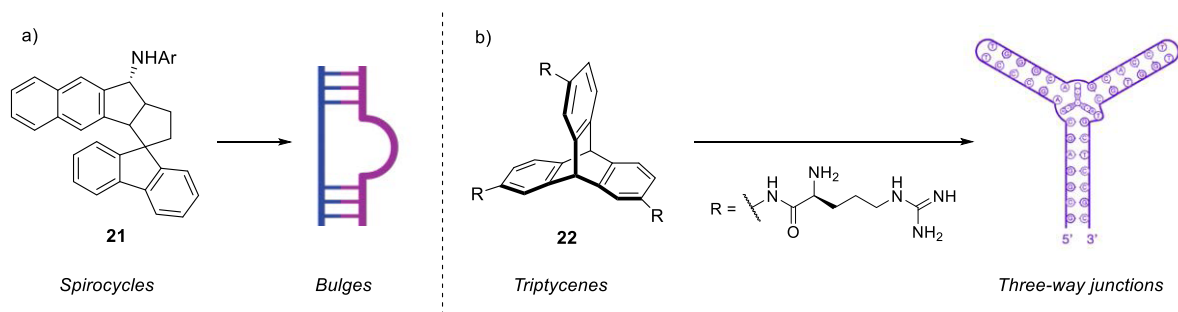
the evaluation of the Gibbs free energy for potential photoinduced electron-transfer processes. According to this analysis, ET from the excited catalyst to the Hantzsch ester is thermodynamically favorable ($\Delta G_{\text{ET}} = -0.63$ eV). Conversely, direct ET from the excited state of **9b** to substrate **19a** is thermodynamically disfavored ($\Delta G_{\text{ET}} = +0.13$ eV). Furthermore, UV-Vis absorption studies excluded the formation of electron donor-acceptor (EDA) complexes, as no appreciable spectral changes were detected upon gradual addition of either **19a** or **21** to a solution of **9b**. Finally, the reaction was shown to halt immediately upon interruption of light irradiation, thereby excluding the involvement of a self-propagating radical chain process in the photocleavage mechanism.

Based on the collected experimental data, the photodesulfonylation was proposed to proceed via the mechanism illustrated in Scheme 7.

Upon irradiation at 300 nm, pCp-based catalyst **9b** is promoted to its excited state (**A**), which then undergoes a single-electron transfer (SET) with the Hantzsch ester. This step generates dihydropyridine radical cation **C** and coumarin-centered radical anion **B**. The radical anion subsequently interacts with the reaction substrate, forming radical in-

termediate **D** and regenerating the ground-state photocatalyst. Note that the formation of intermediate **D** aligns with analogous species previously identified in related electrochemical processes [82]. Radical **D** then undergoes homolytic cleavage of its N-S bond, yielding carboxamide anion **E** and aryl sulfonyl radical ArSO_2^\bullet . The final desulfonylated product is formed through quenching reactions between these species and dihydropyridine radical cation **C**. The proposed mechanistic pathway was further corroborated by theoretical calculations carried out in collaboration with A. Maruani (LCBPT UPCit ).

Attaining precise control over chirality in photoinduced organic transformations remains one of the foremost challenges in the field of photocatalysis. While numerous reports have demonstrated satisfactory enantioselectivities using costly transition-metal-based catalysts [83], there is growing interest in metal-free strategies. These approaches often employ chiral organocatalysts that function dually as stereocontrolling agents and photosensitizers [84–86]. Despite these advances, examples of asymmetric photocatalytic reactions driven by such organocatalysts remain scarce [87]. Building on this background, our current research is focused on investigating enantiopure planar chiral pCp derivatives



Scheme 8. Examples of three-dimensional ligands preferentially targeting non-paired RNA structures.

heat shock response in *E. coli*, highlighting their functional relevance as RNA-targeting agents. The non-planar architecture of these molecules, which arranges aromatic groups across orthogonal planes, appears to mitigate non-specific intercalation into double-helical regions. This spatial configuration enhances selectivity for non-duplex RNA motifs while minimizing off-target interactions with double-stranded DNA, thus overcoming a common limitation of planar aromatic RNA-binding compounds.

Inspired by these precedents, we hypothesized that pCps could preferentially drive recognition of non-helical RNA structural motifs. Indeed, their rigid and sterically demanding architecture, characterized by a 3.1 Å distance between the benzene moieties (Figure 1), does not match the helical rise per base pair in double-stranded RNA (2.6 Å) or DNA (3.4 Å), making intercalation unlikely and effectively limiting interactions with RNA or DNA duplexes (Figure 6).

Guided by this rationale, we explored pCp as a central core for the design of novel RNA-binding ligands. Simultaneously, we aimed to exploit the intrinsic photophysical properties of pCps to monitor ligand–RNA interactions via fluorescence spectroscopy, enabling real-time observation of binding events.

Cyanine dyes are well-established probes in chemical biology, frequently used for nucleic acid staining [60,101,102]. These dyes exhibit strong fluorescence turn-on behaviors upon target binding. We therefore set out to compare the luminescence responses of pCp-based cyanine dye **12** with those of analogous flat cyanine **13** in the presence of nucleic acids.

As described earlier in this article, both compounds exhibited low emission in aqueous buffer

(Table 3). However, upon the addition of increasing amounts of tRNA, a significant fluorescence enhancement was observed for both cyanines, demonstrating that incorporation of the pCp moiety into the luminophore does not negatively impact the turn-on behavior of the cyanine (Figure 7) [59].

Digestion studies with RNase A confirmed that the observed fluorescence enhancement is attributable to the presence of RNA in solution [34]. Since cyanines are known to form aggregates [61]—a tendency also confirmed for pCp derivative **12**—, the observed turn-on responses were attributed to disaggregation processes triggered by the interaction of the dyes with RNA.

We next compared the behavior of the flat and three-dimensional cyanines in the presence of different types of nucleic acids. Interestingly, flat compound **13** exhibited comparable fluorescence turn-on responses with all tested nucleic acids (Figure 8, in red), indicating a non-selective interaction profile. In contrast, three-dimensional pCp-based derivative **12** displayed only modest fluorescence enhancements in the presence of double-stranded DNA or RNA (Figure 8, in blue), while it showed markedly stronger turn-on behaviors with nucleic acids containing multiple unpaired regions, with a clear preference for tRNA.

Fluorescence titrations performed with custom-designed hairpin loops of different sizes (I–V, Table 6) further demonstrated that pCp-based dye **12** interacts weakly with small loop structures, while exhibiting higher binding affinity—reflected by lower dissociation constants (K_d)—for larger loops. Remarkably, the dye showed a marked preference for a sequence containing eight unpaired nucleotides ($K_d \sim 0.54 \mu\text{M}$, Table 6). It is also worth noting that, at this

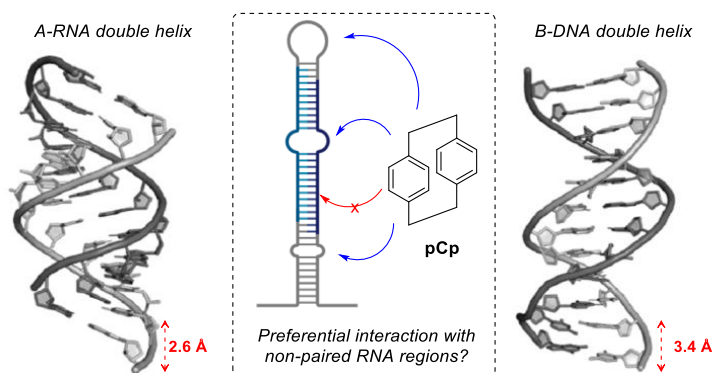


Figure 6. Rationale for targeting non-paired RNA motifs using pCp.

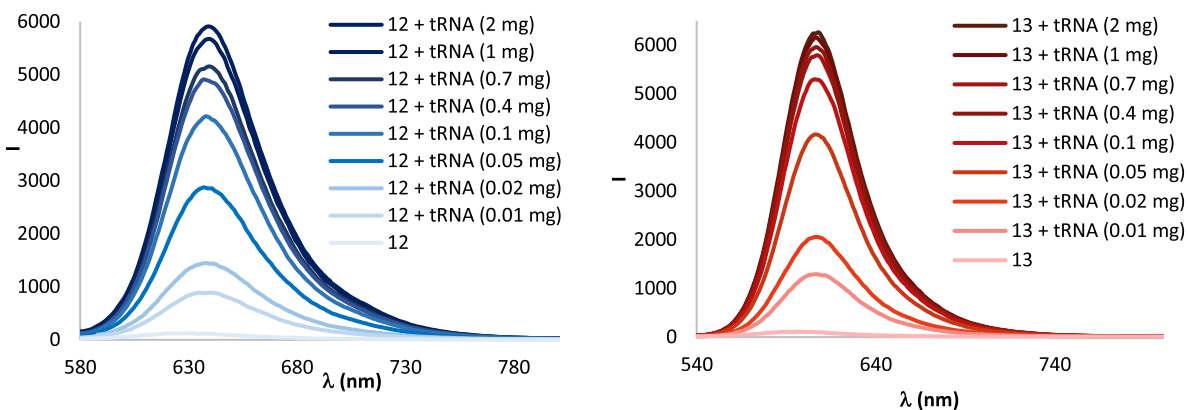


Figure 7. Turn-on fluorescence responses of cyanines **12** (in blue) and **13** (in red) in the presence of increasing amounts of tRNA.

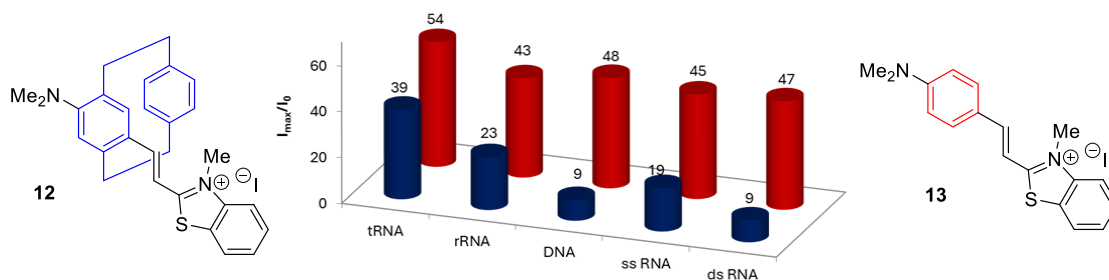
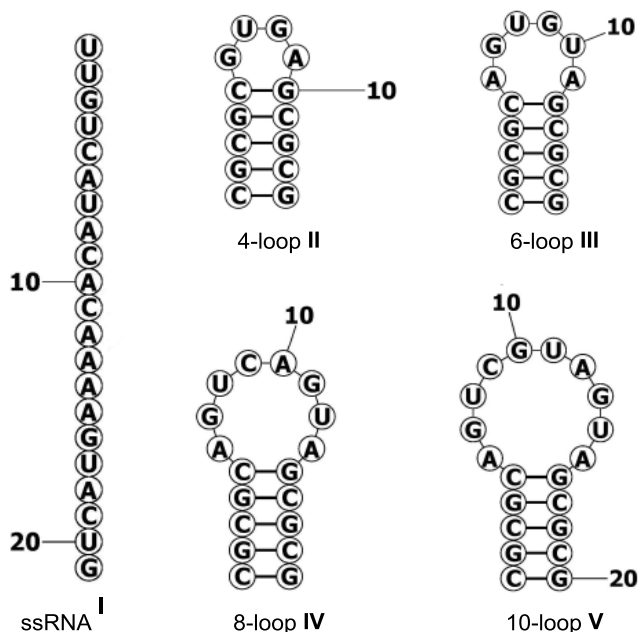


Figure 8. Turn-on fluorescence responses of cyanines **12** and **13** (10^{-6} M) in the presence of diverse nucleic acid (0.4 mg/mL) in Tris-EDTA (TE) buffer at 20 °C.

Table 6. Dissociation constants (μM) for RNA–cyanine **12** interactions

I ^a	II ^a	III ^a	IV ^b	V ^b
14.22	24.53	6.04	0.54	1.65
± 14.46	± 6.60	± 2.05	± 0.16	± 1.14

^a 10^{-6} M solution of dye **12** in Tris-EDTA (TE) buffer. ^b 10^{-7} M solution of dye **12** in Tris-EDTA (TE) buffer. Data are presented as mean of the three independent experiments \pm standard deviation.

stage, both racemic and enantiopure compounds exhibited similar behavior [34].

In the future, the ability of enantiopure pCp-based luminophores to emit circularly polarized luminescence may be harnessed to monitor RNA–ligand interactions via CPL spectroscopy. This approach may offer several advantages, including enhanced sensitivity and selectivity stemming from the polarized nature of the emitted light, reduced background interference relative to conventional fluorescence methods, and the potential to provide detailed insights into the chiral environment and binding-induced conformational changes of RNA structures.

8. Conclusions

Thanks to their unique three-dimensional geometry, distinctive electronic properties, and atypical reactivity, [2.2]paracyclophanes (pCps) have emerged as

versatile molecular platforms attracting growing interest across diverse areas of chemical research.

In this account, we have highlighted a variety of strategies that enable the selective functionalization of their aromatic cores, efficient control over planar chirality, and modulation of their photophysical properties. The methods developed in our laboratory have enabled access to structurally diverse pCp scaffolds with tunable spectroscopic behaviors on synthetically useful scales. These rigid π -stacked systems exhibited significant potential in fields such as organic and organometallic luminophore chemistry, photocatalysis, and chemical biology. Nevertheless, important challenges remain to be addressed. For example, the development of selective functionalization protocols targeting the ethylene bridges and the *meta* or *pseudo-meta* positions of these scaffolds could greatly broaden their chemical diversity. Strategies to further modulate the

absorption and emission properties of functionalized pCps, such as attaining higher brightness and enhanced CPL efficiency, also warrant continued investigation. In lanthanide chemistry, pCp-based ligands with planar chirality may lead to the development of next-generation luminescent and multimodal metal complexes. The use of enantiopure chiral pCp derivatives as photosensitizers in photoredox catalysis also remains underexplored and could enable the design of novel light-activated asymmetric transformations. Finally, our recent efforts to incorporate the pCp motif into RNA-binding small molecules have opened promising avenues for targeting non-paired structural motifs within nucleic acids. However, further studies are required to better elucidate the precise binding mode of pCp derivatives to RNA.

In summary, pCps represent a fascinating class of molecular architectures that continue to captivate the chemistry community. Despite the significant progress already achieved in their synthesis and controlled functionalization, we are confident that ongoing research on these original compounds will continue to drive innovation across a range of disciplines, including organic synthesis, materials science, and chemical biology.

Acknowledgments

The authors extend their sincere thanks to all undergraduate, master's, and PhD students, as well as postdoctoral researchers and collaborators, for their invaluable contributions. Special thanks are due to J. Crassous, L. Favereaux, and F. Pointillart (Univ. Rennes 1); O. Maury and L. Abad-Galan (ENS Lyon); A. Maruani, S. Lajnef, F. Peyrot, C. Sagné and S. Turcaud (Paris Cité University).

Declaration of interests

The authors do not work for, advise, own shares in, or receive funds from any organization that could benefit from this article, and have declared no affiliations other than their research organizations.

Funding

The authors gratefully acknowledge the support of the CNRS and Paris Cité University (*IdEx Dynamique*

Recherche pCp-Photocat - ANR-18-IDEX-0001), as well as funding from the *Agence Nationale de la Recherche (ANR JCJC PhotoChiraPhane - ANR-19-CE07-0001-01)*.

References

- [1] C. J. Brown and A. C. Farthing, "Preparation and structure of di-p-xylylene", *Nature* **164** (1949), pp. 915–916.
- [2] H. Hope, J. Bernstein and K. N. Trueblood, "Trueblood, The crystal and molecular structure of 1,1,2,2,9,9,10,10-octafluoro-[2,2]paracyclophane and a reinvestigation of the structure of [2,2]paracyclophane", *Acta Cryst. B* **28** (1972), pp. 1733–1743.
- [3] S. Wu, S. Felder, J. Brom, F. Pointillart, O. Maury, L. Micouin and E. Benedetti, "[2.2] paracyclophanes: From selective functionalization to optical properties", *Adv. Optical Mater.* **12** (2024), article no. 2400934.
- [4] H. E. Winberg, F. S. Fawcett, W. E. Mochel and C. W. Theobald, "Dimethylenedihydroheteroaromatic compounds and heterocyclophanes by 1,6-Hofmann elimination reactions", *J. Am. Chem. Soc.* **82** (1960), pp. 1428–1435.
- [5] M. Brink, "Eine verbesserte synthese von [2.2]paracyclophan und 4-formyl-[2.2]paracyclophan", *Synthesis* **12** (1975), pp. 807–808.
- [6] T. Otsubo and V. Boekelheide, "An alternate route for the conversion of dithia[3.3]cyclophanes to cyclophane-dienes. Reaction with benzyne followed by sulfoxide pyrolysis", *Tetrahedron Lett.* **45** (1975), pp. 3881–3884.
- [7] A. Iwama, T. Toyoda, M. Yoshida, T. Otsubo, Y. Sakata and S. Misumi, "Layered compounds. LII. Syntheses of eleven anthracenophanes", *Bull. Chem. Soc. Jpn.* **51** (1978), pp. 2988–2994.
- [8] M. Montanari, A. Bugana, A. K. Sharma and D. Pasini, "Mild preparation of functionalized [2.2] paracyclophanes via the Pummerer rearrangement", *Org. Biomol. Chem.* **9** (2011), pp. 5018–5020.
- [9] J. Lahann, D. Klee and H. Höcker, "Chemical vapour deposition polymerization of substituted [2.2] paracyclophanes", *Macromol. Rapid Commun.* **19** (1998), pp. 441–444.
- [10] H. Nandivada, H.-Y. Chen, L. Bondarenko and J. Lahann, "Reactive polymer coatings that "click"", *Angew. Chem. Int. Ed.* **45** (2006), pp. 3360–3363.
- [11] H. Pu, Y. Wang and Z. Yang, "Chemical vapor deposition copolymerization of 4-carboxyl-[2, 2] paracyclophane and 4-amino-[2, 2] paracyclophane", *Mater. Lett.* **61** (2007), pp. 2718–2722.
- [12] Z. Hassan, D. Varadharajan, C. Zippel, S. Begum, J. Lahann and S. Bräse, "Design strategies for structurally controlled polymer surfaces via cyclophane-based CVD polymerization and post-CVD fabrication", *Adv. Mater.* **34** (2022), article no. 2201761.
- [13] D. Klee, N. Weiss and J. Lahann, in *Modern Cyclophane Chemistry* (R. Gleiter and H. Hopf, eds.), Wiley-VCH: Weinheim, 2004, pp. 463–484.

- [14] Z. Hassan, E. Spuling, D. M. Knoll and S. Bräse, "Regioselective functionalization of [2.2] paracyclophanes: Recent synthetic progress and perspectives", *Angew. Chem. Int. Ed.* **59** (2020), pp. 2156–2170.
- [15] J. Pu, L. Chen, R.-R. Wu, et al., "Non-directed Pd-catalysed C–H arylation of [2.2] paracyclophane", *Chem. Commun.* **59** (2023), pp. 9348–9351.
- [16] M.-L. Delcourt, S. Felder, S. Turcaud, C. H. Pollok, C. Merten, L. Micouin and E. Benedetti, "Highly enantioselective asymmetric transfer hydrogenation: a practical and scalable method to efficiently access planar chiral [2.2] paracyclophanes", *J. Org. Chem.* **84** (2019), pp. 5369–5382.
- [17] S. H. Eltamany and H. Hopf, "Cyclophane, XIV: darstellung polymethylierter [2.2] paracyclophane", *Tetrahedron Lett.* **21** (1980), pp. 4901–4904.
- [18] Y. Zhao, X. Li, W.-H. Deng, B. Wu, R.-Z. Liao and Y.-G. Zhou, "Dearomatization of [2.2]paracyclophane-derived N-sulfonylimines through cyclopropanation with sulfur ylides", *J. Org. Chem.* **89** (2024), pp. 321–329.
- [19] D. Ly, J. Bacs and H. M. L. Davies, "Rhodium (II)-catalyzed asymmetric cyclopropanation and desymmetrization of [2.2] paracyclophanes", *ACS Catal.* **14** (2024), pp. 6423–6431.
- [20] N. V. Vorontsova, E. V. Vorontsov, E. V. Sergeeva and V. I. Rozenberg, "The first regioselective double electrophilic substitution of the C2-symmetric pseudo-metadibstituted [2.2] paracyclophanes", *Tetrahedron Lett.* **47** (2006), pp. 2357–2360.
- [21] K. P. Javasundera, D. N. M. Kusmus, L. Deuillhé, L. Etheridge, Z. Farrow, D. J. Lun, G. Kaur and G. J. Rowlands, "The synthesis of substituted amino [2.2] paracyclophanes", *Org. Biomol. Chem.* **14** (2016), pp. 10848–10860.
- [22] S. Felder, L. Micouin and E. Benedetti, "Para-functionalization of N-substituted 4-amino [2.2] paracyclophanes by regioselective formylation", *Eur. J. Org. Chem.* **2021** (2021), pp. 4015–4018.
- [23] S. E. Walden and D. T. Glatzhofer, "Distinctive normal harmonic vibrations of [2.2] paracyclophane", *J. Phys. Chem. A* **101** (1997), pp. 8233–8241.
- [24] D. Henseler and G. Hohlneicher, "Theoretical study on the molecular distortions in [2.2] paracyclophane and cyclobutene", *J. Phys. Chem. A* **102** (1998), pp. 10828–10833.
- [25] S. Grimme and C. Mück-Lichtenfeld, "Accurate computation of structures and strain energies of cyclophanes with modern DFT methods", *Isr. J. Chem.* **52** (2012), pp. 180–192.
- [26] R. S. Cahn, C. Ingold and V. Prelog, "Specification of molecular chirality", *Angew. Chem. Int. Ed.* **5** (1966), pp. 385–415.
- [27] D. J. Cram and N. L. Allinger, "Macro rings. XII. Stereochemical consequences of steric compression in the smallest paracyclophane", *J. Am. Chem. Soc.* **77** (1955), pp. 6289–6294.
- [28] S. E. Gibson and J. D. Knight, "[2.2] Paracyclophane derivatives in asymmetric catalysis", *Org. Biomol. Chem.* **1** (2003), pp. 1256–1269.
- [29] Y. Morisaki and Y. Chujo, "Planar chiral [2.2] paracyclophanes: optical resolution and transformation to optically active π -stacked molecules", *Bull. Chem. Soc. Jpn.* **92** (2019), pp. 265–274.
- [30] K. J. Weiland, A. Gallego and M. Mayor, "Beyond simple substitution patterns—Symmetrically tetrasubstituted [2.2] paracyclophanes as 3D functional materials", *Eur. J. Org. Chem.* **2019** (2019), pp. 3073–3085.
- [31] S. Felder, S. Wu, J. Brom, L. Micouin and E. Benedetti, "Enantiopure planar chiral [2.2] paracyclophanes: Synthesis and applications in asymmetric organocatalysis", *Chirality* **33** (2021), pp. 506–527.
- [32] M.-L. Delcourt, S. Turcaud, E. Benedetti and L. Micouin, "Efficient and scalable kinetic resolution of racemic 4-formyl[2.2]paracyclophane via asymmetric transfer hydrogenation", *Adv. Synth. Catal.* **358** (2016), pp. 1213–1215.
- [33] M.-L. Delcourt, S. Felder, E. Benedetti and L. Micouin, "Highly enantioselective desymmetrization of centrosymmetric pseudo-paradiformyl[2.2]paracyclophane via asymmetric transfer hydrogenation", *ACS Catal.* **8** (2018), pp. 6612–6616.
- [34] Z. Wu, S. Fang, J. He, J. Che, Z. Liu, X. Wei, Z. Su and T. Wang, "Desymmetrization/kinetic resolution of planar chiral [2.2] paracyclophanes by bioinspired peptide-aminophosphorane catalysis", *Angew. Chem. Int. Ed.* **64** (2025), article no. e202423702.
- [35] V. Docekal, F. Koucky, I. Cisarova and J. Vesely, "Organocatalytic desymmetrization provides access to planar chiral [2.2] paracyclophanes", *Nat. Commun.* **15** (2024), article no. 3090.
- [36] S. Yu, H. Bao, D. Zhang and X. Yang, "Kinetic resolution of substituted amido [2.2] paracyclophanes via asymmetric electrophilic amination", *Nat. Commun.* **14** (2023), article no. 5239.
- [37] Y. Zhao, Y.-X. Ding, B. Wu and Y.-G. Zhou, "Nickel-catalyzed asymmetric hydrogenation for kinetic resolution of [2.2]paracyclophane-derived cyclic N-sulfonylimines", *J. Org. Chem.* **86** (2021), pp. 10788–10798.
- [38] C. Zippel, Z. Hassan, A. Q. Parsa, J. Hohmann and S. Braese, "Multigram-scale kinetic resolution of 4-acetyl[2.2]paracyclophane via Ru-catalyzed enantioselective hydrogenation: Accessing [2.2]paracyclophanes with planar and central chirality", *Adv. Synth. Catal.* **363** (2021), pp. 2861–2865.
- [39] S.-C. Huo, R. R. Indurmuddam, B.-C. Hong, C.-F. Lua and S.-Y. Chien, "The hamburger-shape photocatalyst: thioxanthone-based chiral [2.2]paracyclophane for enantioselective visible-light photocatalysis of 3-methylquinoxalin-2(1H)-one and styrenes", *Org. Biomol. Chem.* **21** (2023), pp. 9330–9336.
- [40] P. Rademacher, in *Modern Cyclophane Chemistry* (R. Gleiter and H. Hopf, eds.), Wiley-VCH: Weinheim, 2004, pp. 275–310.
- [41] D. J. Cram, N. L. Allinger and H. Steinberg, "Macro rings. VII. The spectral consequences of bringing two benzene

- rings face to face", *J. Am. Chem. Soc.* **76** (1954), pp. 6132–6141.
- [42] G. C. Bazan, W. J. Oldham, R. J. Lachicotte, S. Tretiak, V. Chernyak and S. Mukamel, "Stilbenoid dimers: dissection of a paracyclophane chromophore", *J. Am. Chem. Soc.* **120** (1998), pp. 9188–9204.
- [43] G. P. Bartholomew and G. C. Bazan, "Bichromophoric paracyclophanes: models for interchromophore delocalization", *Acc. Chem. Res.* **34** (2001), pp. 30–39.
- [44] W. J. Oldham, Y. J. Miao, R. J. Lachicotte and G. C. Bazan, "Stilbenoid dimers: effect of conjugation length and relative chromophore orientation", *J. Am. Chem. Soc.* **120** (1998), pp. 419–420.
- [45] J. Zyss, I. Ledoux, S. Volkov, V. Chernyak, S. Mukamel, G. P. Bartholomew and G. C. Bazan, "Through-space charge transfer and nonlinear optical properties of substituted paracyclophane", *J. Am. Chem. Soc.* **122** (2000), pp. 11956–11962.
- [46] Y. Liu and P. Xing, "Circularly polarized light responsive materials: Design strategies and applications", *Adv. Optical Mater.* **35** (2023), article no. 2300968.
- [47] A. Yanagawa, M. Tsuchiya, R. Inoue and Y. Morisaki, "Optical resolution of pseudo-para-disubstituted [2.2]paracyclophane: a chiral building block for optically active helicene-stacked molecules emitting circularly polarized luminescence", *J. Mater. Chem. C* **11** (2023), pp. 986–993.
- [48] Y. Morisaki, M. Gon, T. Sasamori, N. Tokitoh and Y. Chujo, "Planar chiral tetrasubstituted [2.2] paracyclophane: optical resolution and functionalization", *J. Am. Chem. Soc.* **136** (2014), pp. 3350–3353.
- [49] Y. Morisaki, K. Inoshita and Y. Chujo, "Planar-chiral through-space conjugated oligomers: Synthesis and characterization of chiroptical properties", *Chem. Eur. J.* **20** (2014), pp. 8386–8390.
- [50] Y. Morisaki, R. Hifumi, L. Lin, K. Inoshita and Y. Chujo, "Through-space conjugated polymers consisting of planar chiral pseudo-ortho-linked [2.2] paracyclophane", *Polym. Chem.* **3** (2012), pp. 2727–2730.
- [51] M. Gon, Y. Morisaki and Y. Chujo, "Optically active cyclic compounds based on planar chiral [2.2] paracyclophane: extension of the conjugated systems and chiroptical properties", *J. Mater. Chem. C* **3** (2015), pp. 521–529.
- [52] M. Gon, H. Kozuka, Y. Morisaki and Y. Chujo, "Optically active cyclic compounds based on planar chiral [2.2] paracyclophane with naphthalene units", *Asian J. Org. Chem.* **5** (2016), pp. 353–359.
- [53] M. Gon, Y. Morisaki and Y. Chujo, "Highly emissive optically active conjugated dimers consisting of a planar chiral [2.2] paracyclophane showing circularly polarized luminescence", *Eur. J. Org. Chem.* **2015** (2015), pp. 7756–7762.
- [54] M. Gon, Y. Morisaki, R. Sawada and Y. Chujo, "Synthesis of optically active, x-shaped, conjugated compounds and dendrimers based on planar chiral [2.2]paracyclophane, leading to highly emissive circularly polarized luminescence", *Chem. Eur. J.* **22** (2016), pp. 2291–2298.
- [55] A. Morisaki, R. Inoue and Y. Morisaki, "Synthesis of two novel optically active #-shaped cyclic tetramers based on planar chiral [2.2] paracyclophanes", *Chem. Eur. J.* **29** (2023), article no. e202203533.
- [56] X. Li, Y. Xie and Z. Li, "The progress of circularly polarized luminescence in chiral purely organic materials", *Adv. Photonics Res.* **2** (2021), article no. 2000136.
- [57] S. Felder, M.-L. Delcourt, D. Contant, R. Rodríguez, L. Favereau, J. Crassous, L. Micouin and E. Benedetti, "Compact CPL emitters based on a [2.2] paracyclophane scaffold: recent developments and future perspectives", *J. Mater. Chem. C* **11** (2023), pp. 2053–2062.
- [58] M.-L. Delcourt, C. Reynaud, S. Turcaud, L. Favereau, J. Crassous, L. Micouin and E. Benedetti, "3D Coumarin systems based on [2.2] paracyclophane: Synthesis, spectroscopic characterization, and chiroptical properties", *J. Org. Chem.* **84** (2019), pp. 888–899.
- [59] S. Felder, C. Sagné, E. Benedetti and L. Micouin, "Small-molecule 3D ligand for RNA recognition: tuning selectivity through scaffold hopping", *ACS Chem. Biol.* **17** (2022), pp. 3069–3076.
- [60] N. Akbay, M. Y. Losytskyy, V. B. Kovalska, A. O. Balanda and S. M. Yarmoluk, "The mechanism of benzothiazole styrylcyanine dyes binding with dsDNA: Studies by spectral-luminescent methods", *J. Fluoresc.* **18** (2008), pp. 139–147.
- [61] J.-C. G. Bünzli, "On the design of highly luminescent lanthanide complexes", *Coord. Chem. Rev.* **293–294** (2015), pp. 19–47.
- [62] J.-C. G. Bünzli, "Lanthanide luminescence for biomedical analyses and imaging", *Chem. Rev.* **110** (2010), pp. 2729–2755.
- [63] G.-Q. Jin, Y. Ning, J.-X. Geng, Z.-F. Jiang, Y. Wang and J.-L. Zhang, "Joining the journey to near infrared (NIR) imaging: the emerging role of lanthanides in the designing of molecular probes", *Inorg. Chem. Front.* **7** (2020), pp. 289–299.
- [64] O. Guillou, C. Daiguebonne, G. Calvez and K. Bernot, "A long journey in lanthanide chemistry: From fundamental crystallography studies to commercial anticounterfeiting taggants", *Acc. Chem. Res.* **49** (2016), pp. 844–856.
- [65] S. I. Weissman, "Intramolecular energy transfer the fluorescence of complexes of europium", *J. Chem. Phys.* **10** (1942), pp. 214–217.
- [66] H. Uh and S. Petoud, "Novel antennae for the sensitization of near infrared luminescent lanthanide cations", *C. R. Chim.* **13** (2010), pp. 668–680.
- [67] Z. Hassan, E. Spuling, D. M. Knoll, J. Lahann and S. Bräse, "Planar chiral [2.2] paracyclophanes: from synthetic curiosity to applications in asymmetric synthesis and materials", *Chem. Soc. Rev.* **47** (2018), pp. 6947–6963.
- [68] R. Grykien, B. Luszczynska, I. Glowacki, et al., "Electric field tunable light emitting diodes containing europium β -diketonates with [2.2] paracyclophane moiety", *Opt. Mater.* **57** (2016), pp. 114–119.
- [69] S. Wu, L. A. Galan, M. Roux, et al., "Tuning excited-state properties of [2.2] paracyclophane-based antennas to ensure efficient sensitization of lanthanide ions or singlet oxygen generation", *Inorg. Chem.* **60** (2021), pp. 16194–16203.

- [70] R. Marin, G. Brunet and M. Murugesu, "Shining new light on multifunctional lanthanide single-molecule magnets", *Angew. Chem. Int. Ed.* **60** (2021), pp. 1728–1746.
- [71] K. Bernot, "Get under the umbrella: A comprehensive gateway for researchers on lanthanide-based single-molecule magnets", *Eur. J. Inorg. Chem.* **26** (2023), article no. e202300336.
- [72] D. N. Woodruff, R. E. P. Winpenny and R. A. Layfield, "Lanthanide single-molecule magnets", *Chem. Rev.* **113** (2013), pp. 5110–5148.
- [73] D. Thakura and S. Vaidyanathan, "Chiral lanthanide complexes in the history of circularly polarized luminescence: a brief summary", *J. Mater. Chem. C* **13** (2025), pp. 9410–9452.
- [74] F. Pointillart, M. Atzori and C. Train, "Magnetochiroism of chiral lanthanide complexes", *Inorg. Chem. Front.* **11** (2024), pp. 1313–1321.
- [75] H. Flichot, A. Sickinger, J. Brom, et al., "Magnetochiroism correlation in lanthanide luminescent [2.2] paracyclophane-based single-molecule magnets", *Dalton Trans.* **53** (2024), pp. 8191–8201.
- [76] G. Ciamician, "The photochemistry of the future", *Science* **36** (1912), pp. 385–394.
- [77] P. Melchiorre, "Introduction: photochemical catalytic processes", *Chem. Rev.* **122** (2022), pp. 1483–1484.
- [78] J. Xuan, B.-J. Li, Z.-J. Feng, et al., "Desulfonylation of tosyl amides through catalytic photoredox cleavage of N-S bond under visible-light irradiation", *Chem. Asian J.* **8** (2013), pp. 1090–1094.
- [79] A. Gualandi, G. Rodeghiero, E. Della Rocca, et al., "Application of coumarin dyes for organic photoredox catalysis", *Chem. Commun.* **54** (2018), pp. 10044–10047.
- [80] A. Gualandi, A. Nenov, M. Marchini, et al., "Tailored coumarin dyes for photoredox catalysis: Calculation, synthesis, and electronic properties", *ChemCatChem* **13** (2021), pp. 981–989.
- [81] J. Brom, A. Maruani, S. Turcaud, S. Lajnef, F. Peyrot, L. Micouin and E. Benedetti, "[2.2] Paracyclophane-based coumarins: effective organo-photocatalysts for light-induced desulfonylation processes", *Org. Biomol. Chem.* **22** (2024), pp. 59–64.
- [82] P. Viaud, V. Coeffard, C. Thobie-Gautier, I. Beaudet, N. Galland, J.-P. Quintard and E. Le Grogne, "Electrochemical cleavage of sulfonamides: an efficient and tunable strategy to prevent β -fragmentation and epimerization", *Org. Lett.* **14** (2012), pp. 942–945.
- [83] A. J. David, R. Balaji and A. Das, "Advances of chiral metal complexes as standalone photocatalyst for asymmetric organic transformations", *Adv. Synth. Catal.* **367** (2025), article no. e202401543.
- [84] A. Bauer, F. Westkamper, S. Grimme and T. Bach, "Catalytic enantioselective reactions driven by photoinduced electron transfer", *Nature* **436** (2005), pp. 1139–1140.
- [85] C. Muller, A. Bauer and T. Bach, "Light-driven enantioselective organocatalysis", *Angew. Chem. Int. Ed.* **48** (2009), pp. 6640–6642.
- [86] J. Großkopf, T. Kratz, T. Rigotti and T. Bach, "Enantioselective photochemical reactions enabled by triplet energy transfer", *Chem. Rev.* **122** (2022), pp. 1626–1653.
- [87] C. Prentice, J. Morrisson, A. D. Smith and E. Zysman-Colman, "Recent developments in enantioselective photocatalysis", *Beilstein J. Org. Chem.* **16** (2020), pp. 2363–2441.
- [88] X. Cao, Y. Zhang, Y. Ding and Y. Wan, "Identification of RNA structures and their roles in RNA functions", *Nat. Rev. Mol. Cell Biol.* **25** (2024), pp. 784–801.
- [89] V. Bernat and M. D. Disney, "RNA structures as mediators of neurological diseases and as drug targets", *Neuron* **87** (2015), pp. 28–46.
- [90] A. Fatica, "The emerging role of RNA in diseases and cancers", *Int. J. Mol. Sci.* **24** (2023), article no. 6682.
- [91] J. L. Childs-Disney, X. Yang, Q. M. R. Gibaut, Y. Tong, R. T. Batey and M. D. Disney, "Targeting RNA structures with small molecules", *Nat. Rev. Drug Discov.* **21** (2022), pp. 736–762.
- [92] Y. Tong, J. L. Childs-Disney and M. D. Disney, "Targeting RNA with small molecules, from RNA structures to precision medicines: IUPHAR review: 40", *Br. J. Pharmacol.* **181** (2024), pp. 4152–4173.
- [93] A. E. Hargrove, "Small molecule–RNA targeting: starting with the fundamentals", *Chem. Commun.* **56** (2020), pp. 14744–14756.
- [94] S. Kovachka, M. Panosetti, B. Grimaldi, S. Azoulay, A. Di Giorgio and M. Duca, "Small molecule approaches to targeting RNA", *Nat. Rev. Chem.* **8** (2024), pp. 120–135.
- [95] K. Deigan Warner, C. E. Hajdin and K. M. Weeks, "Principles for targeting RNA with drug-like small molecules", *Nat. Rev. Drug Discov.* **17** (2018), pp. 547–558.
- [96] S. T. Meyer and P. J. Hergenrother, "Small molecule ligands for bulged RNA secondary structures", *Org. Lett.* **11** (2009), pp. 4052–4055.
- [97] C. Fleurisson, N. Graidia, J. Azzouz, et al., "Design and Evaluation of Azaspirocycles as RNA binders", *Chem. Eur. J.* **31** (2025), article no. e202403518.
- [98] S. A. Barros and D. M. Chenoweth, "Triptycene-based small molecules modulate (CAG)–(CTG) repeat junctions", *Chem. Sci.* **6** (2015), article no. 4752.
- [99] S. A. Barros and D. M. Chenoweth, "Recognition of nucleic acid junctions using triptycene-based molecules", *Angew. Chem. Int. Ed.* **53** (2014), pp. 13746–13750.
- [100] S. A. Barros, I. Yoon and D. M. Chenoweth, "Modulation of the *E. coli* rpoH temperature sensor with triptycene-based small molecules", *Angew. Chem. Int. Ed.* **55** (2016), pp. 8258–8261.
- [101] V. B. Kovalska, D. V. Kryvorotenko, A. O. Balanda, M. Yu Losytskyy, V. P. Tokar and S. M. Yarmoluk, "Fluorescent homodimer styrylcyanines: synthesis and spectral-luminescent studies in nucleic acids and protein complexes", *Dyes Pigm.* **67** (2005), pp. 47–54.
- [102] C.-Q. Zhu, S.-J. Zhuo, H. Zheng, J.-L. Chen, D.-H. Li, S.-H. Li and J.-G. Xu, "Fluorescence enhancement method for the determination of nucleic acids using cationic cyanine as a fluorescence probe", *Analyst* **129** (2004), pp. 254–258.